Toxicon:X 23 (2024) 100199

Contents lists available at ScienceDirect

Toxicon: X

journal homepage: www.journals.elsevier.com/toxicon-x

Cyanotoxin accumulation and growth patterns of biocrust communities under variable environmental conditions

Aspassia D. Chatziefthimiou [a,b,*,1], James S. Metcalf [c,d], William B. Glover [c], James T. Powell [c], Sandra A. Banack [c], Paul A. Cox [c], Moncef Ladjimi [a], Ali A. Sultan [a], Hiam Chemaitelly [a], Renee A. Richer [e]

[a] Weill Cornell Medicine – Qatar, Education City, Doha, Qatar
[b] Independent Researcher, Doha, Qatar
[c] Brain Chemistry Labs, Institute for Ethnomedicine, Jackson, WY, USA
[d] Bowling Green State University, Bowling Green, OH, USA
[e] Duke Kunshan University, Kushan, China

ARTICLE INFO

Handling editor: Ray Norton

Keywords:
Biocrusts
Cyanobacteria
Cyanotoxins
Desertification
Climate change
BMAA

ABSTRACT

Biocrusts dominate the soil surface in deserts and are composed of diverse microbial communities that provide important ecosystem services. Cyanobacteria in biocrusts produce many secondary metabolites, including the neurotoxins BMAA, AEG, DAB, anatoxin-a(*S*) (guanitoxin), and the microcystin hepatotoxins, all known or suspected to cause disease or illness in humans and other animals. We examined cyanobacterial growth and prevalence of these toxins in biocrusts at millimeter-scales, under a desert-relevant illumination gradient. In contrast to previous work, we showed that hydration had an overall positive effect on growth and toxin accumulation, that nitrogen was not correlated with growth or toxin production, and that phosphorus enrichment negatively affected AEG and BMAA concentrations. Excess illumination positively correlated with AEG, and negatively correlated with all other toxins and growth. Basic pH negatively affected only the accumulation of BMAA. Anatoxin-a(*S*) (guanitoxin) was not correlated with any tested variables, while microcystins were not detected in any of the samples. Concerning toxin pools, AEG and BMAA were good predictors of the presence of one another. In a newly conceptualized scheme, we integrate aspects of biocrust growth and toxin pool accumulations with arid-relevant desertification drivers.

1. Introduction

Biological Soil Crusts (biocrusts) cover the top centimeters of most soils in drylands across the globe, and are comprised of a plethora of microbial partners (Belnap, 2003). Biocrusts play an essential role in desert system dynamics because they are the primary providers of ecosystem services and influence soil fertility, plant succession, and overall biodiversity (Belnap et al., 2005; Liu et al., 2017). Soil fertility services include soil stability, increasing moisture retention potential, soil respiration, and nutrient cycling. These services are quite important considering that 31% of the world's population reside in desert ecosystems and many of them depend upon arid areas for their food production and livelihood (Hori et al., 2011; Prăvălie, 2016; IPCC, 2019). Furthermore, since drylands cover up to 41–45% of the Earth's land area, biocrusts may have a large effect on climate regulation including carbon sequestration and solar radiance absorption (Prăvălie, 2016; Faist et al., 2017).

Biocrust community composition is shaped by both climatic and anthropogenic factors. Early successional communities are made up by autotrophic and heterotrophic bacteria as well as light-colored photosynthetic cyanobacteria, while dark-colored pigmented cyanobacteria, lichens and mosses are dominant in later successional stages (Garcia-Pichel et al., 2003; Pepe-Ranney et al., 2015). Climatic stress factors, such as low precipitation and high evapotranspiration, jointly defined as Aridity Index (AI), may partly account for the early successional biocrusts observed in countries like Qatar with low AIs (AI < 0.03; Chatziefthimiou et al., 2016) compared to late successional ones in some of the hot deserts of the Western USA, for example, with higher AIs (0.03 <

* Corresponding author. Weill Cornell Medicine – Qatar, Education City, PO Box 24114, Doha, Qatar.
E-mail address: a.d.chatziefthimiou@gmail.com (A.D. Chatziefthimiou).
[1] Current address at: PO Box 22880, Doha, Qatar.

https://doi.org/10.1016/j.toxcx.2024.100199
Received 12 March 2024; Received in revised form 28 May 2024; Accepted 29 May 2024
Available online 6 June 2024

AI < 0.65; Hori et al., 2011). Anthropogenic stress factors include land degradation or habitat loss from development, as well as two corollaries of climate change: unpredictability of precipitation patterns and increased albedo from human-generated hardscape. Such stress factors can cause depletion of soil nutrients and loss of fertile and bio-active land, a process termed desertification, which is a global-scale issue since all ecosystems across climatic regions are vulnerable to it, not just the drylands (MEA, 2005; Hori et al., 2011). Depending on the intensity of stress (disturbance), biocrust communities may return to earlier stages of succession and cyanobacterial dominance, or be wiped out completely, thus ceasing primary productivity and essential ecosystem services altogether. This can have grave consequences since biocrusts are sometimes the sole providers of these services in drylands (Ferrenberg et al., 2015).

Biocrust communities are adept at responding to environmental stress and maintain their ecosystem services, in part, through an armory of secondary metabolites that cyanobacteria produce (Metcalf and Codd 2012; Powell et al., 2015). These increase their fitness and resilience under stress, but if kept unchecked, exposure to these same secondary metabolites may pose a threat to ecosystem, human and animal health in drylands. In biocrusts in the Qatari desert, where their land cover may reach up to 87% in certain areas (Richer et al., 2012), the secondary metabolites β-N-methylamino-L-alanine (BMAA), and isomers 2,4-diaminobutyric acid (DAB), N-2(aminoethyl)glycine (AEG), as well as anatoxin-a(*S*) (guanitoxin; Fiore et al., 2020), all shown to act as neurotoxins, have consistently been detected (Cox et al., 2009, 2016; Chatziefthimiou et al., 2014; Metcalf et al., 2015; Martin et al., 2019; Schneider et al., 2020), along with the hepatotoxic microcystins (Metcalf et al., 2012; Powell et al., 2015).

Toxin exposure routes for humans and other animals, may occur in drylands through the consumption of toxin-contaminated seafood (AEG and DAB; Chatziefthimiou et al., 2018), and through consumption of toxin-contaminated potable water from storage tanks, groundwater wells and rain pools (AEG, DAB, microcystins, and anatoxin-a(*S*) (guanitoxin); Chatziefthimiou et al., 2014, 2016). Exposure to aerosolized BMAA from physically disturbed biocrusts via inhalation, was hypothesized to be a cause of the time-limited spike of Amyotrophic Lateral Sclerosis (ALS) cases a decade after the 1990–1991 Operations Desert Shield and Desert Storm in military personnel that were deployed to the Arabian Peninsula compared to personnel with the same training who were not deployed (Horner et al., 2003; Cox et al., 2009). It has been shown that exposure to BMAA induces the development of amyloid deposits and neurofibrillary tangles, hallmarks of neurodegenerative diseases, in primates (*Chlorocebus sabaeus*; Cox et al., 2016). In this model, evidence of motor neuron degeneration was identified through activated microglia, reactive astrogliosis, TDP-43^{+} proteinopathy in anterior horn cells, and damage to myelinated axons in the lateral corticospinal tracts, all characteristic of preclinical ALS/motor neuron disease (Davis et al., 2020). The toxicity of BMAA to human cells was also noted to increase when co-exposed with known isomers (Martin et al., 2019; Schneider et al., 2020). Inhalation-based exposure to these toxins is a concern considering the vast expanse of drylands and the persistence of BMAA and its isomers in desert ecosystems (Stommel et al., 2013; Richer et al., 2015; Chatziefthimiou et al., 2016, 2020).

In the microbial world, the function of these neurotoxins is not yet fully known, nor are the environmental factors that affect their production. There does appear to be a differential pattern of toxin accumulation that is dependent on the complexity of the microbial community, the environmental conditions, and possibly the type of stress (Downing et al., 2011; Berntzon et al., 2013; Fan et al., 2015; Popova et al., 2018a, b; Koksharova et al., 2020a, 2020b). For example, in pure liquid cultures of cyanobacteria, BMAA accumulated as a response to the stress of nutrient depletion and excessive illumination, which in turn inhibited carbon and nitrogen fixation and upregulated cellular stress response proteins and DNA repair enzymes (Koksharova et al., 2020a, 2020b). On the other hand, in biocrust communities tested in field experiments, the stress from disturbance and desiccation/hydration did not induce an increase in toxin accumulation, even when growth was reduced by 63% (Richer et al., 2015).

With global concerns surrounding the effects of climate change and desertification to the dynamics of ecosystems and drylands in particular, and the health risks associated with toxin exposure, there is a need to better understand growth and toxin accumulation in biocrust communities relative to predictions from climate change models. Although biocrust research is very advanced especially in drylands of the Western USA, the focused line of research on cyanotoxin dynamics within biocrust communities, has solely been conducted in Qatar (Chatziefthimiou et al., 2014, 2016, 2018, 2020; Cox et al., 2009; Metcalf et al., 2012, 2015; Powell et al., 2015; Richer et al., 2015). Available articles and reviews on cyanotoxins in the environment, and/or cyanobacteria in biocrusts in the deserts of the Middle East, refer to that same cluster of publications (Cirés et al., 2017; Dulić et al., 2017, 2022). To add to this line of research, we therefore, tested the hypothesis that toxin accumulation is a cyanobacterial stress response. We predicted increased accumulation of cyanotoxins in biocrusts as a function of decreased growth under a variety of environmental conditions, as suggested by population studies (Downing et al., 2015; Fan et al., 2015). The environmental conditions manipulated were illumination levels (simulating solar radiance), nutrient concentrations and pH levels (simulating change in nitrogen and phosphorus cycles, and soil chemistry due to unpredictability of precipitation patterns; MEA, 2005; Collins and Knutti, 2013; Delgado-Baquerizo et al., 2013). The experiments were conducted in a closed lab-controlled system, under a hydrated state and at a scale relevant to microbial processes measured in millimeters. The specific cyanotoxins that we monitored were BMAA, AEG, DAB, anatoxin-a(*S*) (guanitoxin), and microcystins.

2. Materials and methods

2.1. Field site description, sampling and biocrust characteristics

The field site where samples were collected in January 2014, is a natural depression (rawda) covered with biocrusts dominated by cyanobacteria and devoid of lichens and mosses, located at Al Zubara in Northern Qatar (general coordinates N 25.84502°, E 51.30371°). The average biocrust coverage in this area is the highest in the country (highest 1/3 of ranked means; Richer et al., 2012) and elsewhere reported as being 56% (Cox et al., 2009). Experimental biocrust samples were aseptically collected, using forceps cleaned with 95% ethanol, and stored in sterilized containers to avoid contamination to open air. In the lab, biocrust samples were stored in the dark at room temperature until further analysis as described below.

2.2. Field site environmental and edaphic characteristics

The climate of Qatar is hyper-arid with an Aridity Index (AI) of 0.03 and average evapotranspiration rate of 6 mm per day (MEA, 2005). The mean annual precipitation is 76.3 mm (1972–2013 record), and the Northern part of the country received >110 mm total rainfall in 2013 (MDPS, 2017). The mean annual temperature in Qatar is 32.7 °C with maxima reaching above 45 °C in the dry season between the months of May to September (1962–1992 and 2012 records; MDPS, 2017). Global Horizontal Irradiance (GHI) annual average for Qatar based on satellite-derived data is 222.1 W/m^2 (5.33 kW/m^2/day), with maximum monthly average of 308.3 W/m^2 (7.4 kW/m^2/day) in June (1983–2005 record; SSE, 2017). Ground measurements obtained in 2013 in the Central and Southern parts of Qatar are in agreement with satellite-derivations, while those from the Northern part are significantly higher, with an annual average of 455.9 W/m^2 (10.94 kW/m^2/day) and a maximum monthly average of 599.5 W/m^2 (14.39 kW/m^2/day) in June of that year (MOE, 2014; Perez-Astudillo and Bachour, 2014).

The soil order in Al Zubara is Aridisols, and the soil type is Typic Petrogypsids with a sandy loam texture (MMAA, 2005). The nitrate concentration of the soil is 658.6 ppm NO_3–N (equivalent to 3992 ppm $NaNO_3$), PO_4 is 1–2.82 ppm, and pH exhibits a seasonal variation of 6.8–8.1 where lower values are observed in the winter months (MMAA, 2005).

2.3. Media preparation

BG11 medium (Rippka, 1988) was prepared with three different concentrations of nitrogen and phosphorus, and four pH levels (Table 1). pH measurements were obtained, prior to autoclave-sterilization of the 9 media variations, with a Thermo Scientific™ Orion™ Model 410 pH meter, previously 3-point calibrated with Thermo Scientific™ Orion™ Standard All-in-One™ pH Buffers (Fisher Scientific, Inc., Pennsylvania, USA). The standard concentration of each variable in the gradients when that variable was not tested was 17.6 mM $NaNO_3$, 300 μM $K_2HPO_4 \bullet 3H_2O$, and pH 7 following the standard BG11 medium recipe (Rippka, 1988). To inhibit fungal growth, media preparations were amended post-sterilization with filter-sterilized cyclohexamide solution (0.1 mg/ml, Sigma, Inc., Missouri, USA). All chemicals were obtained from Sigma.

2.4. Experimental set up

A singular piece of biocrust collected from the field site in Al Zubara in Northern Qatar, was aseptically denuded of soil particles, and used to cut cylindrical plugs (8 mm diameter, 1 mm height, volume 50.24 mm^3; flat surface 50.24 mm^2), with a metal hole borer. Plugs were placed in sterilized 19 × 65 mm borosilicate glass vials (Fisher Scientific), with 5 ml of medium. To maintain aseptic conditions, all work was conducted under a laminar flow hood, and aseptic techniques were followed. Each medium variation had triplicate replicates for a total of 81 experimental plugs (Table 1). For uniform light exposure, the sealed vials were positioned horizontally on the bench, and exposed under a Chameleon Plasma Grow Light (Chameleon Grow Systems, Florida, USA) at 3 light intensity regimes to mirror values from ground field measurements and satellite-derivations for the Al Zubara region and to simulate seasonal variation (Fig. 1; Table 1; Perez-Astudilloa and Bachour, 2014; MDPS, 2017; SSE, 2017). Namely, the 3 ranges of light intensity were: 11.1–93.5 W/m^2 to simulate winter and naturally occurring overcast days, 93.5–210.9 W/m^2 to simulate fall and winter seasons, and 210.9–413 W/m^2 to simulate spring and summer seasons. The different light intensities were achieved by hanging the Chameleon Plasma Grow Light at a specific distance from the bench thus creating a gradient of light intensity, measured using a LI-6400XT - Portable Photosynthesis System (LI-COR, Nebraska, USA). The vials were positioned in this gradient according to treatment. For example, the high light regime vials were placed directly under the Chameleon Plasma Grow Light and the low-level light regime vials in the periphery. The distance of the Chameleon Plasma Grow Light was such that heat emitted during exposure did not introduce temperature variability among light regimes. The temperature was maintained between 30.5 and 32 °C throughout the 21-day incubation of the experiment.

Controls were prepared with plugs inoculated in sterilized MilliQ® water (Merck, Massachusetts, USA) and incubated under the 3 different light regimes (Supplementary Material (SM) Table 1). The vials were frequently re-positioned within each of their light regimes throughout the experiment. Finally, another 3 control plugs were incubated for the same duration in complete darkness and in dry conditions with neither

Table 1
Concentrations of nitrate, phosphate and pH levels in BG11 medium and light intensities used in the lab-based experiment with treatments consisting of all combinations of variables.

Experimental Concentration Levels[a]	Treatment				Season of simulation for light intensity
	Nitrate (μM)	Phosphate (mM)	pH	Light intensity (μmole/m^2/s; W/m^2)	
High	17.6	30	10	970 – 1900; 210.9–413	Spring and summer
Medium	0.176	3	8	430 – 970; 93.5–210.9	Fall and winter
Low	0.0176	0.3	6	51 – 430; 11.1–93.5	Winter and normal overcast days
Standard[b]	17.6	229	7	NA[c]	NA[c]

[a] For a description of the controls per experimental treatment, please refer to the experimental set up sub-section.
[b] Standard concentration of BG11 medium (Rippka, 1988) for comparison. pH was adjusted using 0.1 M NaOH.
[c] Not applicable.

Table 2
Frequency of occurrence of cyanotoxins and mean concentrations in experimental biocrust plug samples and controls in relation to light intensity exposure. Each experimental treatment was performed and analyzed in triplicate. Microcystins were not present in any of the analyzed samples.

Light intensity (μmole/m^2/s; W/m^2)	Chlorophyll-a (μg/ml/g)	Total AEG (μg/ml/g)	Total BMAA (μg/ml/g)	Total DAB (μg/ml/g)	Anatoxin-a(*S*) (guanitoxin) (mg/L/g)
	% occurrence (mean concentration; standard deviation)				
High (970–1900; 210.9–413)	96.3 (49.41; ±69.4)	96.3 (0.16; ±0.07)	14.8 (0.03; ±0.01)	100 (0.44; ±0.11)	74.1 (4.07; ±7.5)
Medium (430–970; 93.5–210.9)	96.3 (92.02; ±62.66)	81.5 (0.19; ±0.08)	81.5 (0.06; ±0.04)	70.4 (0.53; ±0.2)	51.9 (25.57; ±11.78)
Low (51–430; 11.1–93.5)	96.3 (105.64; ±72.47)	100 (0.17; ±0.09)	100 (0.08; ±0.05)	100 (0.55; ±0.14)	77.8 (20.37; ±16.65)
Controls No Light, Desiccated	100 (55.82; ±8.12)	33.3 (0.04; ±0.07)	33.3 (0.04; ±0.06)	33.3 (0.22; ±0.39)	0 (0; 0)

Table 3
Summary of levels of light intensity exposure and ecological hierarchy in studies of toxin accumulation.

Light intensity μmole/m^2/s (W/m^2)	Cyanobacteria/Setting	Reference
16 (3.5)	Cyanobacterial populations (*Microcystis* PCC7806, *Synechocystis* J341, and *Synechocystis PCC6803*)/Lab	Downing et al. (2011), and 2012
20 (4.4)	Cyanobacterial populations (*Synechocystis* PCC6803)/Lab	Downing et al. (2015)
36.3 (7.9)	Cyanobacterial populations (*Microcystis aeruginosa* 905 and 315)/Lab	Fan et al. (2015)
51 (11.1)	Biocrust mixed communities/Lab	Present study
108.9 (23.7)	Cyanobacterial populations (*Microcystis aeruginosa* 905 and 315)/Lab	Fan et al. (2015)
217.8 (47.4)	Cyanobacterial populations (*Microcystis aeruginosa* 905 and 315)/Lab	Fan et al. (2015)
326.7 (71.1)	Cyanobacterial populations (*Microcystis aeruginosa* 905 and 315)/Lab	Fan et al. (2015)
430 (93.5)	Biocrust mixed communities/Lab	Present study
825.2 (179.6)[a]	Biocrust mixed communities/Field	Richer et al. (2015)
970 (210.9)	Biocrust mixed communities/Lab	Present study
1900 (413)	Biocrust mixed communities/Lab	Present study

[a] Extrapolated from the 1983–2005 record for Global Horizontal Irradiance for Qatar (SSE 2017) for the months of October/November, when this study took place.

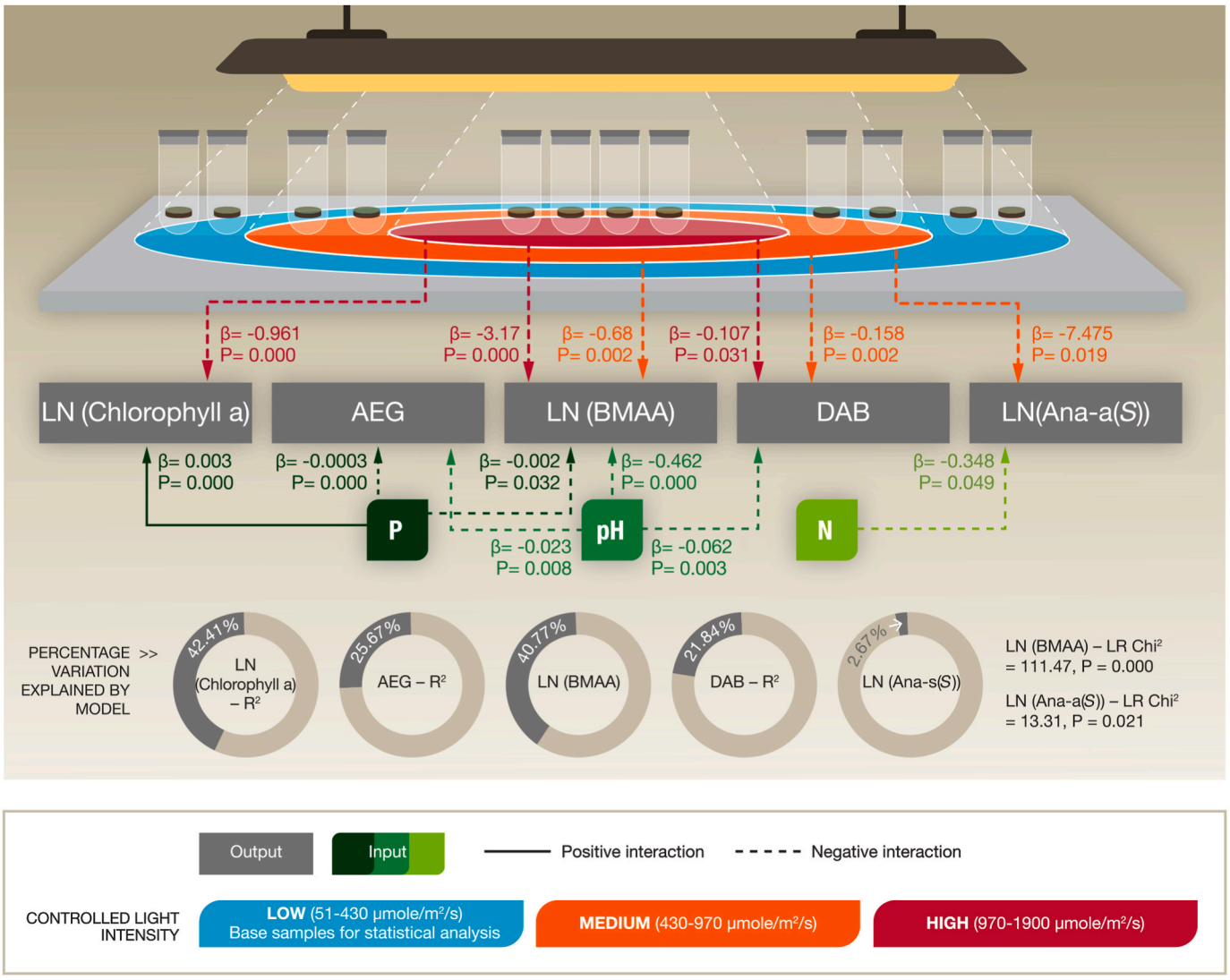

Fig. 1. Schematic diagram of the effect of abiotic variables on the growth of biocrusts and toxin accumulation. Toxins were not considered as variables in this statistical model. Only statistically significant associations (P-value <0.050) are depicted in this figure. Percent variation explained by this model is expressed in R^2 for chlorophyll-a (proxy of growth) as well as for the toxins AEG and DAB, and pseudo R^2 for toxins BMAA and anatoxin-a(*S*) (guanitoxin). For BMAA and anatoxin-a (*S*) (guanitoxin) the goodness-of-fit for the statistical models was performed using the Likelihood Ratio Chi^2 test.

medium amendments nor sterilized MilliQ® water.

2.5. Microscopic examination of biocrust communities

The standard method of microscopy was used to identify actively growing cyanobacteria in biocrusts. Sub-samples were fixed using 20% ethanol or Lugol's iodine and observed under a light microscope. Samples were assessed using a Zeiss Axioplan 2 (Zeiss, San Diego, CA, USA) using light and fluorescence microscopy, the latter with excitation between 515 and 560 nm (green) and emission at 580 nm (red) using a 100W mercury vapor lamp. Cyanobacteria in the sub-samples were identified to genus level, using taxonomic classification guidelines according to Whitton (2002).

2.6. Harvest

Each experimental vial was centrifuged at 14,000×*g* for 3 min (Eppendorf 5417R; Eppendorf AG, Hamburg, Germany) on day 21 and the spent medium was removed. Each pelleted plug was lyophilized in a LabConco FreeZone® Plus™ 4.5 L Cascade Console Freeze Dry System (LabConco, Missouri, USA) overnight, and was subsequently cut aseptically in 3 pieces, weighed, and kept at – 80 °C until analyzed for chlorophyll-a and toxins.

2.7. Chlorophyll-a extraction and analysis

Chlorophyll-a, used as a proxy for cyanobacterial growth, was extracted from lyophilized biocrust plug sub-samples, using 90% acetone (Sigma, Inc., Missouri, USA) at concentrations of 0.4–1.1 g (dry wt.)/ml, followed by overnight incubation in the dark at 4 °C (SCOR–UNESCO, 1966). Sub-samples were centrifuged at maximum speed (Eppendorf 5417R; Eppendorf AG, Hamburg, Germany) and 0.2 ml of the supernatant were transferred to a microtiter plate. Absorbance was measured using a PowerWave XS Microplate Spectrophotometer (BioTek®, Vermont, USA), at wavelengths of 630, 645, 663 and 750 nm. The absorbance reading at 750 nm was subtracted from all the other readings, and chlorophyll *a* concentration was calculated in µg/g of biocrust sub-sample using the equation: $11.64(A_{663}) - 2.16(A_{645}) + 0.1(A_{630})$.

2.8. Toxin extractions

Microcystins and anatoxin-a(*S*) (guanitoxin) from lyophilized plug sub-samples were extracted sequentially in 100% and 70% methanol (Sigma) with ultrasonication at an amplitude of 40% using a Fisher Scientific™ Model 120 Sonic Dismembrator (Fisher Scientific; Metcalf et al., 2006; Chatziefthimiou et al., 2016). Although 70–75% methanol has been used for the efficient extraction of microcystins from freeze-dried cyanobacterial matrices (Ward et al., 1997; Fastner et al., 1998), using such solvents with biocrusts resulted in an inability to obtain a supernatant. Therefore, 100% methanol was used to extract cyanotoxins as this provided a supernatant which also had the potential to extract free toxins present within voids of soil and rock, in addition to being capable of extracting microcystins (e.g., Ward et al., 1997).

Extraction protocols for AEG, BMAA and DAB followed Richer et al. (2015). In more detail here, a lyophilized sub-sample of each experimental and control plug, was weighed and placed in a 10 ml sterile borosilicate glass vial (Fisher Scientific). One milliliter of 6 M hydrochloric acid (HCl; Sigma) was added to each vial, and these were subsequently placed in a Digital Dry Block Heater (VWR, Georgia, USA) to hydrolyze the sub-samples at 110 °C for 16 h. The vials were left to cool down, and 0.2 ml of the supernatant were transferred in a 0.22 μm pore size Ultrafree®-MC Centrifugal Filter (Merck KGaA, Darmstadt, Germany), centrifuged at 12,000 rpm for 4 min (Eppendorf AG). The filters were discarded, and the filtered supernatant was dried into a pellet at 45 °C for 3h in a Speed Vac (Fisher Scientific). The tubes were sealed with parafilm and stored at – 80 °C until they were analyzed.

2.9. Toxin analyses

Microcystins were quantified using the Acquity ultra performance liquid chromatography system (Waters Corp., Massachusetts, USA) with photodiode array (PDA) detection at 238 nm (Metcalf et al., 2006). Anatoxin-a(*S*) (guanitoxin) analyses were performed using a colorimetric acetylcholine esterase inhibition assay (Mahmood and Carmichael, 1987). Extracts for the analysis of AEG, BMAA and DAB were rehydrated with 20 mM HCl and derivatized with 6-aminoquinolyl-N--hydroxysuccinimidyl carbamate and analyzed using Ultra High Performance Liquid Chromatography with single quadrupole mass spectrometric detection (UHPLC-MS) and a second generation heated electrospray probe (H-ESI) as described in full elsewhere (Richer et al., 2015; Chatziefthimiou et al., 2016). In brief, separation of isomers was achieved using a Waters AccQTag Ultra column (part# 186003837, 2.1 # 100 mm) heated to 55 °C along with a gradient elution (Eluent A: 0.1% (v/v) formic acid in water (Fisher Optima W6-1, #28905); Eluent B: 0.1% (v/v) formic acid in acetonitrile (Eluent B, Honeywell Burdick & Jackson #LC441–2.5); 0.0 min 99.1% A; 0.5 min 99.1% A curve 6; 2 min 95% A curve 6; 3 min 95% A curve 6; 5.5 min 90% A curve 8; 6 min 15% A curve 6; 6.5 min 15% A curve 6; 6.6 min 99.1% A curve 6; 8 min 99.1% A curve 6. Detection was achieved using selective reaction monitoring (SRM) with m/z 459 (M + H) and m/z 230 (M+2H).

During toxin analyses, purified standards (where available), internal standards and reagent and solvent blanks were used as part of the analytical QC procedures. Limits of detection (LOD) and quantification (LOQ) for BMAA isomers were 0.01 ng/ml and 0.04 ng/ml respectively (Banack, 2021), for microcystins these were 0.1 and 0.02 μg/ml, respectively, and as no anatoxin-a(*S*) (guanitoxin) standards are available, neostigmine was used for comparison of the acetylcholine esterase inhibitory activity of the extracts.

2.10. Statistical analysis

For statistical analysis purposes, a lowest value was assigned to all samples for AEG, BMAA, DAB and anatoxin-a(*S*) (guanitoxin) when their levels were below the detection limit. The lowest value for AEG, BMAA, and DAB was calculated by dividing the Not Detected (ND) limit concentration of each toxin (AEG and BMAA $\leq$0.018 μg/ml, and DAB $\leq$0.070 μg/ml) with the biocrust plug weight of each sample and multiplying by the proportion of hydrolysate volume used for the lyophilization (Supplementary Material (SM) Table 1). For anatoxin-a (*S*) (guanitoxin), the ND limit ($\leq$0.102 μg/ml) was divided by the weight of the lyophilized biocrust plug sample because this toxin's extract was not lyophilized, but instead dried up and re-suspended in an appropriate solvent for analysis (See section on toxin extraction above). After this adjustment, values were sorted, and the lowest value was used uniformly across the ND samples of each toxin (AEG = 0.0087 μg/g, BMAA = 0.0057 μg/g, DAB = 0.03387 μg/g and anatoxin-a(*S*) (guanitoxin) = 1.13×10^{-7} mg/g). Microcystins were not included in any of the statistical analyses as they were not detected in any of the experimental biocrust plugs.

Scatter plots examined the distribution of the outcomes (chlorophyll-a, AEG, DAB, BMAA and anatoxin-a(*S*) (guanitoxin)) with respect to each experimental variable (light intensity, nitrogen, phosphorus, and pH). Log transformations were subsequently applied to chlorophyll-a, BMAA and anatoxin-a(*S*) (guanitoxin) to meet normality assumptions. For all statistical analyses, the low level of light exposure was used as the base value for medium and high light intensities. Bivariate linear regression analyses were performed to examine the association between each experimental variable and chlorophyll-a, AEG, and DAB, respectively (SM Table 2). For BMAA and anatoxin-a(*S*) (guanitoxin), bivariate tobit regression analyses examined their association with each experimental variable adjusting for the left censoring in the data of these toxins (SM Table 2; McDonald and Moffit, 1980). Multivariate linear and tobit regression models incorporating all experimental variables at once, were also used to assess the relative contribution of each variable to the observed levels of chlorophyll-a, AEG, DAB, BMAA and anatoxin-a(*S*) (guanitoxin), respectively (Model 1; SM Table 3). Finally, multivariate linear and tobit regression analyses incorporating all experimental variables and all outcomes at once, were performed to examine the relative contribution of each to the observed levels of chlorophyll-a, AEG, DAB, BMAA and anatoxin-a(*S*) (guanitoxin; Model 2; SM Table 4). P-values are reported and tested for each association at the level of significance of 0.05. All analyses were performed using STATA/SE version 13.0 (StataCorp, 2013).

3. Results

Four experimental variables (illumination, nitrogen, phosphorus and pH) were examined with respect to photosynthetic growth, measured using chlorophyll-a, and the production of the 4 neurotoxins (BMAA, AEG, DAB, anatoxin-a(*S*) (guanitoxin)) and the hepatotoxic microcystins previously found in hydrated biocrust sub samples. Here, chlorophyll-a and the 5 toxins are collectively called outcomes. Two multivariate statistical models were tested, the first in order to evaluate the interplay between these variables and their contribution to the outcomes (Model 1; Fig. 1), and a second one to evaluate the contribution to all outcomes by both the environmental variables and the outcomes themselves (Model 2; Fig. 2).

3.1. Biocrust community composition

The core cyanobacterial community in the experimental biocrust, identified by light microscopy according to standard texts was comprised of the filamentous genera *Lyngbya*, *Microcoleus*, *Nostoc*, *Oscillatoria* and *Phormidium*, along with *Gloeocapsa* and other chroococcalean cyanobacteria (Fig. 3).

3.2. Influence of desiccation/hydration on growth and toxin accumulation

All treatments were kept under the same hydration conditions representing rainfall occurring during different seasons with variable

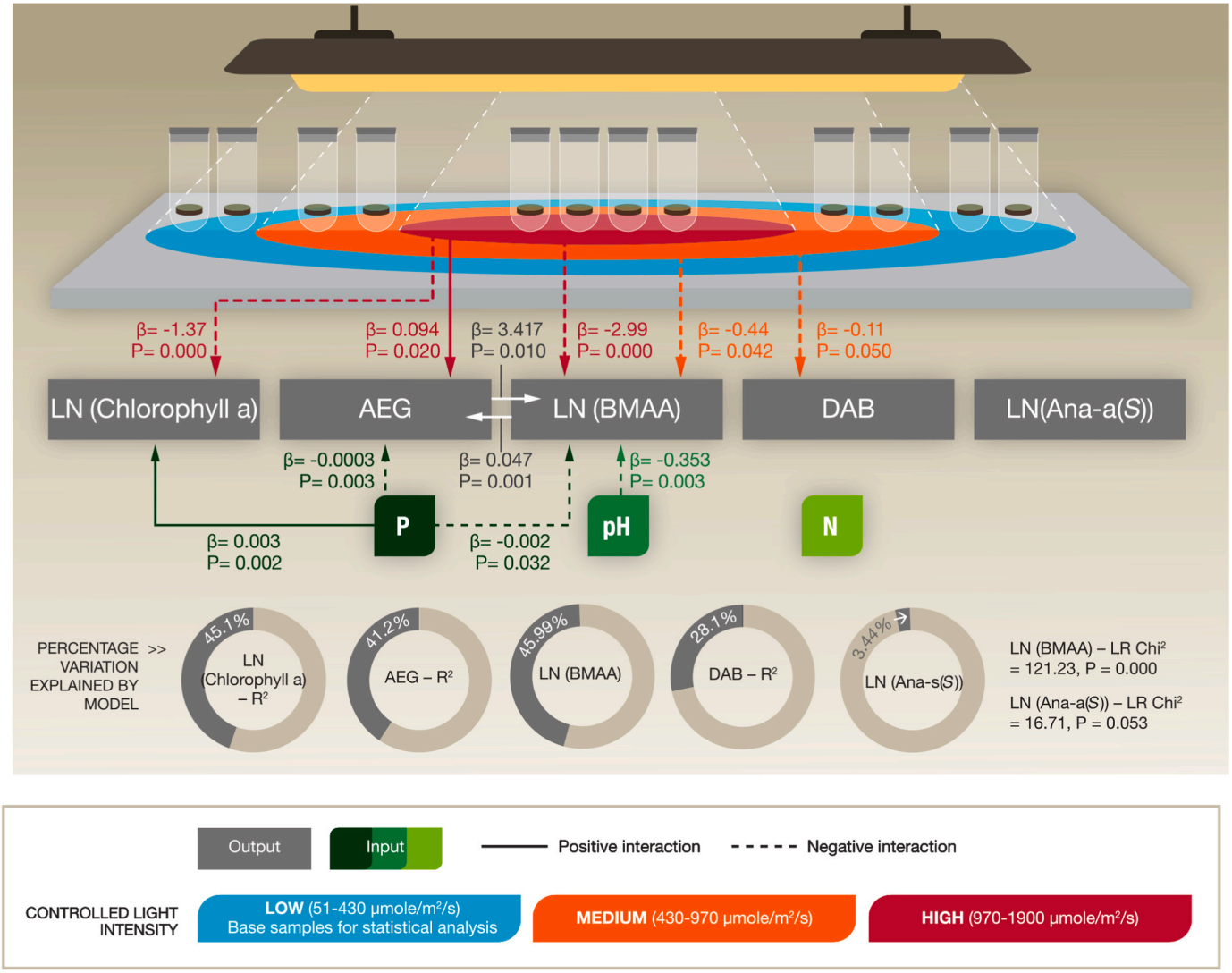

Fig. 2. Schematic diagram of the effect of abiotic variables and toxins on the growth of biocrusts and toxin accumulation. Toxins were included as variables in this model. Only statistically significant associations (P-value <0.050) are depicted in this figure, except for nitrogen and anatoxin-a(*S*) (guanitoxin), which are included here for comparison purposes with Fig. 1. Percent variation explained by this model is expressed in R^2 for chlorophyll-a (proxy of growth) as well as for the toxins AEG, BMAA and DAB. For the toxin BMAA the goodness-of-fit for the statistical models was performed using the Likelihood Ratio Chi^2 test.

nutrient and light availability (Table 1). Control samples

were measured after conditions of both hydration and light but without nutrients, as well as under conditions of desiccation with no light or nutrient amendments (SM Table 1). Chlorophyll-a, used as a proxy for growth, was present in all biocrust plug controls. The hydrated controls with light but no nutrients had less Chlorophyll-a concentration (mean = 30.2 µg/ml/g) compared to those kept in the dark and without water (mean = 55.8 µg/ml/g) suggesting the importance of nutrient input within this system for biological growth. Growth was, on average, 32.2% higher in the illuminated (averaged light intensities) and hydrated experimental biocrust plug samples in comparison to the desiccated, dark control group (Table 2; SM Table 1). BMAA, AEG and DAB, were all found in desiccated/dark controls, and when exposed to illumination and hydration, their concentration increased on average by 37.1%, 75.7%, and 55.9% respectively. Microcystins and anatoxin-a(*S*) (guanitoxin), were below the detection limits in desiccated/dark controls. Anatoxin-a(*S*) (guanitoxin) was detected in 67.9% of the illuminated and hydrated experimental biocrust samples with the highest concentrations under the complete nutrient-absent conditions of the hydrated controls (high and low light intensities only; SM Table 1). Microcystins were not detected in any experimental sample.

3.3. *Effect of light intensity on growth and toxin accumulation*

Chlorophyll-a and toxin analyses of the biocrust plug samples, revealed variable patterns of growth and toxin accumulation in relation to light intensity (Table 2; SM Table 1). Although growth occurred equally under all light regimes (96.3 %), the mean concentration of chlorophyll-a was decreased to half under the high light regime (H: 49.41 µg/ml/g) when compared to the low light regime (L: 105.64 µg/ml/g) (Table 2; SM Table 1). This was corroborated by both statistical models for LN(chlorophyll-a) with statistical significance (P-value = 0.000; Figs. 1 and 2; SM Tables 3 and 4).

Toxin accumulation was also lowest (mean concentrations) under the high light, yet responses to medium (M) and low light regimes were not uniform across the tested toxins. BMAA percent occurrence (L: 100%, M: 81.5%, H: 14.8%; Table 2; SM Table 1) and accumulation (mean concentration L: 0.08 µg/ml/g, M: 0.06 µg/ml/g, H: 0.03 µg/ml/g; Table 2; SM Table 1) were both inversely proportional to intensity of light, decreasing incrementally as light intensity increased, a finding supported for LN(BMAA) by both statistical models (Model 1: H: β = – 3.17, P-value = 0.000, M: β = - 0.68, P-value = 0.002; Model 2: H: β = – 2.99, P-value = 0.000, M: β = - 0.44, P-value = 0.042; Figs. 1 and 2; SM

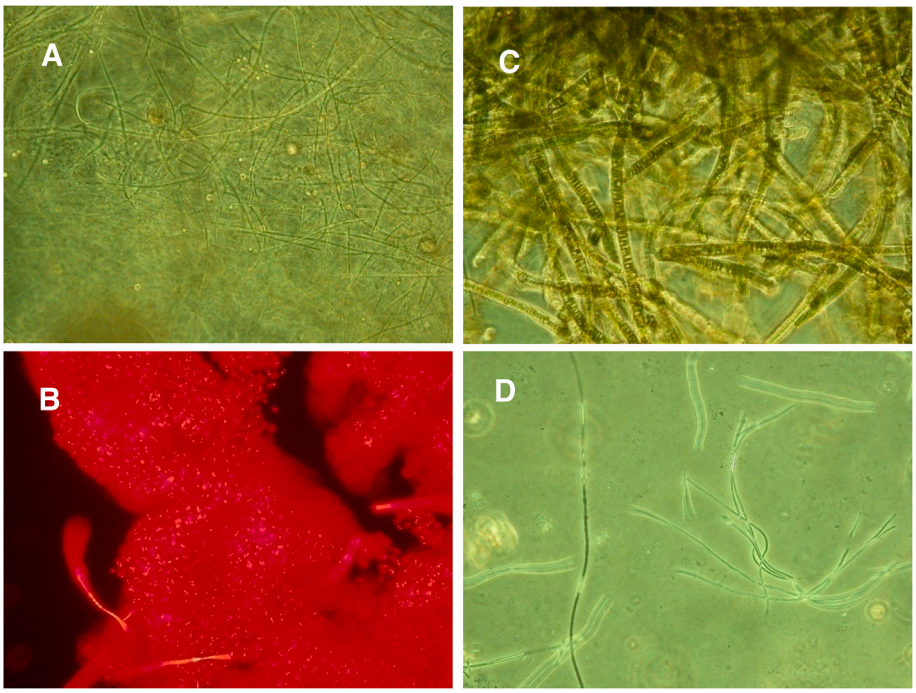

Fig. 3. Example photomicrographs of cyanobacteria found in biocrust samples. A: *Microcoleus* sp. B: chroococcalean cyanobacteria under fluorescence microscopy. C: hetetrocyst-forming cyanobacterium (Nostocales). D: members of the Oscillatoriales.

Tables 3 and 4).

The isomer DAB, mirrored BMAA's inversely proportional mean concentration accumulation pattern, but reached levels of 7–17 orders of magnitude higher than BMAA at low to high light intensity. This differential in DAB accumulation is supported by the statistical Model 1 (H: $\beta = -0.107$, P-value = 0.031, M: $\beta = -0.158$, P-value = 0.002; Fig. 1; SM Table 3), yet when all outcomes were incorporated in Model 2, DAB's association with the high light collapses, while the negative association with the medium light remains (M: $\beta = -0.11$, P-value = 0.050; Fig. 2; SM Table 4), something that is reflected by the steep decrease in DAB's percent occurrence pattern as well (L: 100%, M: 70.4%, L: 100%; Table 2; SM Table 1).

Mean concentrations of the BMAA isomer AEG (L: 0.17 μg/ml/g, M: 0.19 μg/ml/g, H: 0.16 μg/ml/g; Table 2; SM Table 1) peaked under medium light, although the percent occurrence of AEG in those samples was the lowest, i.e., AEG was not consistently produced by all tested biocrust plug samples under this light treatment (L: 100%, M: 81.5%, H: 96.3%; Table 2; SM Table 1). This was not supported by either Model 1, as there were no associations between light intensity and AEG (Fig. 1; SM Table 3), nor by Model 2, where AEG had a statistically significant and positive association to high light (H: $\beta = 0.094$, P-value = 0.020; Fig. 2; SM Table 4) and not to medium light where its accumulation peaked. Mean concentrations of AEG were 2.5–6.3 orders of magnitude higher than BMAA at low to high light intensity, respectively.

Anatoxin-a(*S*) (guanitoxin) showed similar patterns to AEG, with mean concentrations (L: 20.37 mg/L/g, M: 25.57 mg/L/g, H: 4.07 mg/L/g; Table 2; SM Table 1) being the highest at medium light where the lowest percent occurrence was observed (L: 77.8%, M: 51.9%, H: 74.1%; Table 2; SM Table 1). This was not supported by Model 1, where medium light exerted a negative, statistically significant influence on accumulation of LN(Ana-a(*S*)) (M: $\beta = -7.475$, P-value = 0.019; Fig. 1; Table 2; SM Table 3), while in Model 2, all associations with light for anatoxin-a (*S*) (guanitoxin) collapse (Fig. 2; Table 2; SM Table 4).

3.4. Interactions among nutrients, pH, and toxins

The statistical models showed a stark difference in terms of the effect of nutrient availability and pH on growth and toxin accumulation in biocrust plug samples. Nitrogen had no effect on growth or isomer accumulation in either model, and showed only one negative association to LN(Ana-a(*S*)) in Model 1 ($\beta = -0.348$, P-value = 0.049; Fig. 1; SM Table 3), an association that collapsed when all outcomes were incorporated in Model 2 (Fig. 2; SM Table 4). Phosphorus, however, positively affected growth (LN(chlorophyll-a)) in both models (Model 1: $\beta = 0.003$, P-value = 0.000; Model 2: $\beta = 0.003$, P-value = 0.002; Figs. 1 and 2; SM Table 4) and negatively affected AEG in both models (Model 1: $\beta = -0.0003$, P-value = 0.000; Model 2: $\beta = -0.0003$, P-value = 0.003; Figs. 1 and 2; SM Tables 3 and 4). Phosphorus had a negative effect on LN(BMAA) as well, in Model 1 ($\beta = -0.002$, P-value = 0.032; Fig. 1; SM Table 3), an association that collapsed in Model 2 (Fig. 2; SM Table 4). pH was highly influential for the isomers in Model 1 (AEG: $\beta = -0.023$, P-value = 0.008; LN(BMAA): $\beta = -0.462$, P-value = 0.000; DAB: $\beta = -0.062$, P-value = 0.003; Fig. 1; SM Table 3), but for no other factor, while in Model 2 all pH associations collapsed except for that with LN (BMAA) ($\beta = -0.353$, P-value = 0.003; Fig. 2; SM Table 4). Furthermore, in Model 2 there was a bi-directional positive and statistically significant association between AEG ($\beta = 3.417$, P-value = 0.010; Fig. 2; SM Table 4) and LN(BMAA) ($\beta = 0.047$, P-value = 0.001; Fig. 2; SM Table 4), the only association observed among the toxins studied.

Although more factors are interconnected in Model 1 (Fig. 1; SM Table 3), it is by Model 2 (Fig. 2; SM Table 4) that a greater percent of variation was explained for all outcomes, excluding anatoxin-a(*S*) (guanitoxin), while including LN(chlorophyll-a) (Model 1: $R^2 = 42.41\%$; Model 2: $R^2 = 45.1\%$), AEG (Model 1: $R^2 = 25.67\%$; Model 2: $R^2 = 41.2\%$), DAB (Model 1: $R^2 = 21.84\%$; Model 2: $R^2 = 28.1\%$), and LN (BMAA) (Model 1: $R^2 = 40.77\%$; Model 2: $R^2 = 45.99\%$). LN(Ana-a(*S*)) showed a statistically significant goodness-of-fit only for Model 1 (LR $Chi^2 = 13.31$, P-value = 0.021; Fig. 1; SM Table 3).

4. Discussion

This study examined cyanobacterial growth and the concentration of the toxins AEG, BMAA, DAB, anatoxin-a(*S*) (guanitoxin), and microcystins with respect to light, nutrients and pH, in biocrusts monitored in

a closed system and at microbially-relevant scales. During our study, triplicate plugs were analyzed and due to the inherent complex nature of the biocrust soil matrix, variability was high. Consequently, future studies examining toxin production in biocrusts may wish to increase the number of replicate plugs analyzed in anticipation of this complexity.

4.1. Hydration and illumination enhance biocrust community growth and toxin accumulation

Changing global climate conditions can alter biogeochemical cycling. Hydrated controls without added nutrients, following a 21-day lab incubation period, showed reduced growth but similar toxin profiles with the exception of anatoxin-a(*S*) (guanitoxin) which had higher concentrations (SM Table 1). Hydration combined with illumination induced an average 32.2% growth increase, concomitant with 37.1%–75.7% increase in rates of accumulation of all neurotoxins tested, but not for the hepatotoxic microcystins which were not detected in any of the samples pre- or post-treatment (Table 2; SM Table 1).

Ours, contrast findings by Richer et al. (2015), that tested similar treatments in 5-day field experiments in central Al Kharrara area, but only detected AEG and DAB in surface biocrusts, and found no correlation between growth and toxin production. Differences in experimental duration, scales, and design may explain variation in results between studies. And potential leaching of toxins from surface biocrusts into the soil horizon may explain why BMAA was not detected in the field experiments (Chatziefthimiou et al., 2016, 2020).

Differences in the precipitation and solar radiance levels between these sites, may also contribute to differing toxin accumulation responses (Perez-Astudilloa and Bachour, 2014; MDPS, 2017). As is the composition of the toxin producing population that is influenced by environmental conditions as well as priority effects in primary succession (Urban and De Meester, 2009; Mergeay et al., 2011; Andersson et al., 2014), and assembly rules in secondary succession (Lindström and Langenheder, 2012; Schmidt et al., 2014).

Of the cyanotoxins identified in biocrust samples, BMAA, AEG and DAB have the potential to be produced by a wide range of cyanobacteria (Cox et al., 2005; Banack et al., 2010, 2012). With respect to anatoxin-a (*S*) (guanitoxin), currently the only known genera capable of producing are *Dolichospermum* and *Sphaerospermopsis*, order Nostocales (Carmichael and Gorham, 1978; Molica et al., 2005; Fiore et al., 2020). Out of the photosynthetic microorganisms observed by light and fluorescence microscopy in the biocrust sub-samples, *Nostoc*, order Nostocales, was the only genus that may contribute to anatoxin-a(*S*) (guanitoxin) production (Fig. 3). Future studies, using a metagenomics approach, may further clarify cyanobacterial genera capable of producing this toxin in biocrusts.

The results of this study, also deviate from the hypothesis that BMAA and microcystins are interacting stress response factors that regulate growth to preserve functional integrity in cyanobacterial populations (Downing et al., 2015). The different levels of ecological hierarchy among studies may partly account for this, since resilience to stress is expressed uniquely at population and community levels (Table 3; Connell, 1978; Loreau et al., 2001; Bell et al., 2005; Rutherford et al., 2017).

4.2. Illumination and environmental factors induce differential responses in growth and toxin accumulation

Through multivariate linear regression analysis, we assessed the impact of the variables (light intensity, nutrient availability, and pH), on the outcomes (growth and toxin accumulation of biocrust communities), and determined the best predictors of the variability observed in the system. Herewith all toxins are referred to collectively as the “toxin pool”. In Model 1, the impacts are considered in isolation of the outcomes, while in Model 2, the outcomes are integrated in the analysis (Figs. 1 and 2).

In Model 1, we found that high levels of light intensity had detrimental effects on the growth as well as on the accumulation of all toxins except for AEG, which showed no correlation with light intensity (Fig. 1). However, when incorporating the influence of growth and the toxin pool in Model 2, AEG became positively correlated with high light, while the high light correlation with DAB and the medium light correlation for anatoxin-a(*S*) (guanitoxin) collapsed (Fig. 2).

Even though cyanobacteria produce an array of photo-protective pigments against radiation damage, prolonged exposure to radiation can lead to significant mortality (30%–40%; Evans et al., 2001) and loss of metabolic functions (Castenholz and Garcia-Pichel, 2000). Moreover, while pH has been shown to be the best predictor of microbial richness and community composition in soils on a continental scale (Fierer and Jackson, 2006), in our study, phosphorus enrichment and illumination emerged as the best predictors of community growth (Models 1, 2; Figs. 1 and 2).

Previous cyanobacterial population studies have shown that BMAA and DAB accrue as a stress response to excess illumination concomitant with phosphorus enrichment (DAB; Ferrenberg et al., 2015) and nitrogen depletion (Downing et al., 2012; Fan et al., 2015). Here, only AEG accrued under high illumination in Model 2 (Fig. 2), a phenomenon also observed in water samples from sun-exposed water tanks (Chatziefthimiou et al., 2016). Phosphorus enrichment on the other hand, hindered accumulation of both AEG (Model 1, 2; Figs. 1 and 2) and BMAA (Model 1; Fig. 1), while nitrogen depletion singly affected anatoxin-a(*S*) (guanitoxin) (Model 1; Fig. 1) in the absence of growth and the toxin pool influence. Instead, pH being a hub of influence for AEG, BMAA and DAB (Model 1; Fig. 1), is a better predictor of toxin accumulation, in the absence of the outcomes influence.

Lack of corroboration between studies, may lie in the fact that our medium and high desert-relevant light intensities surpass levels of other studies by 1.3–118.8 times (Table 3; Downing et al., 2011, 2012, 2015; Fan et al., 2015). However, when we consider just the lower light intensities uniformly used across studies, the same increased toxin accumulation is observed. Thus, a threshold light-intensity may exist, above which the pool of toxins is diminished, likely through chemical and biological degradation of the existing pool, as has been observed for microcystins (Kormas and Lymperopoulou, 2013), or from biosynthetic machinery malfunctions, as experienced by organisms exposed to extreme conditions (Billi and Potts, 2002).

All factors explored in this study combined, offer more resolution on what drives toxin accumulation in biocrusts than any one in isolation, a resolution that becomes even greater when growth and the toxin pool are considered in Model 2 (Figs. 1 and 2). The residual variation may be explained by factors such as temperature, soil type and texture, % Organic Carbon, % relative humidity, shown previously to predict abundance and diversity of microbial communities (Fierer and Jackson, 2006; Lal, 2011).

4.3. Toxin accumulation exhibits seasonal, and ecosystem-dependent patterns

Studies across hot desert marine and terrestrial ecosystems show a common trend where BMAA, AEG and DAB, are usually detected to a degree of accumulation that is ecosystem dependent, with BMAA being the least abundant and DAB the most (Richer et al., 2015; Chatziefthimiou et al., 2016, 2018, 2020). This seasonal variability has also been shown for anatoxin-a(*S*) (guanitoxin) in biocrusts, yet it is unclear whether the variation is ecosystem driven since this toxin has not been tested across different desert ecosystems (Chatziefthimiou et al., 2014; Metcalf et al., 2012). New analytical methods may provide further insights into this variability and its ecosystem dependency (Dörr et al., 2010). Notably, our study, using different levels of illumination intensity as proxies for seasonal changes (Table 1), mirrors the observed seasonal variability in BMAA isomer ratios in biocrust samples (Figs. 1 and 2).

The understanding of cyanotoxin accumulation in biocrusts and soils is limited (Powell et al., 2015; Chatziefthimiou et al., 2020), hindering

the assessment of whether patterns of toxin accumulation are climate or aridity dependent. Contrastingly, studies on food chains in temperate, tropical and continental climates, have revealed bioaccumulation of BMAA and its isomers up the food chain, with biomagnification up to 11, 000 X in the apex predators as compared to primary producers (Cox et al., 2003; Bell et al., 2005; Brand et al., 2010; Jonasson et al., 2010; Al-Sammak et al., 2014; Büdel et al., 2014; Jiao et al., 2014; Lage et al., 2015; Raggio et al., 2017). In contrast, in arid climates, while bioaccumulation occurs in the marine food chain, biomagnification is absent, and BMAA levels are below the detection limits (Chatziefthimiou et al., 2018). To date, no studies have been conducted to test accumulation patterns of BMAA and its isomers in the terrestrial food chain in deserts.

4.4. Climate change and desertification

Mainly driven by anthropogenic atmospheric increases in CO_2 and other greenhouse gases, climate change puts pressure on thresholds and equilibria of Earth systems decoupling biogeochemical cycles, disrupting ecological interactions and functions, and altering the global energy balance (Fig. 4; Paerl and Huisman 2009; Rockström et al., 2009; Collins and Knutti 2013; Luomi 2016). This study contributes to our understanding of how climate change influences biocrust abundance and succession (Maestre et al., 2012; Rutherford et al., 2017; Fernandes et al., 2018) by examining cyanobacterial growth and cyanotoxin accumulation responses to varying light, nutrient, and pH conditions.

Climate change models predict increased variability in precipitation patterns, either by a shift in the timing of precipitation cycles, or through a reduction in precipitation levels and in the number of wet days, which has the potential to induce drought events (Collins and Knutti, 2013). Drought along with development-driven land degradation, exceptionally rampant in countries of the Middle East, are drivers of desertification (loss of fertile land), which can set in motion a cascade of events that may alter the balance in biogeochemical cycling (Fig. 4; MEA, 2005; Luomi, 2016).

Precipitation stimulates microbial activity in soils which leads to the coupled production of bioavailable nitrogen (N), carbon (C), and phosphorus (P) through its biological liberation from the rock-bound form (Belnap, 2011). Drought on the other hand, stunts microbial activity disrupting the biological control on these biogeochemical cycles, since in the absence of primary productivity, N and C pools become depleted, whereas P is maintained at normal levels by the uninterrupted abiotic weathering of its natural deposits (Delgado-Baquerizo et al., 2013). Another abiotic factor that is correlated with aridity is pH, whereby salts left behind during drought cycles, cause soil salinization, another driver of desertification, making soil pH more basic (MEA, 2005; Hori et al., 2011; Lal, 2011).

During precipitation events, BMAA and AEG are expected to decrease (this study) or remain constant (Richer et al., 2015). It is worthy to note here, that specific to Qatar, these phenomena have already been recorded since the completion of the present experiments, with erratic rain events amassing a year-long rain accumulation (84 mm) in one day (Oct. 2018), followed by severe drought in the following two years (MDPS, 2017; WMO, 2018; QMD, 2021).

Drought induced uncoupling of biogeochemical cycling combined with readily bioavailable P will suppress AEG and BMAA production (Fig. 4), as will basic pH (Fig. 2). If instead, the coupling remains intact with bioavailable N, C, and P all being scarce simultaneously, accumulation of AEG and BMAA is expected to increase as community growth and/or biodiversity decrease. The long-term effect of changing pH on biocrusts may result in a shift in microbial community structure and composition. Under this scenario the toxin profile might change radically and our experiments do not address this possibility. In addition, the presence of BMAA, itself, can affect nitrogen metabolism,

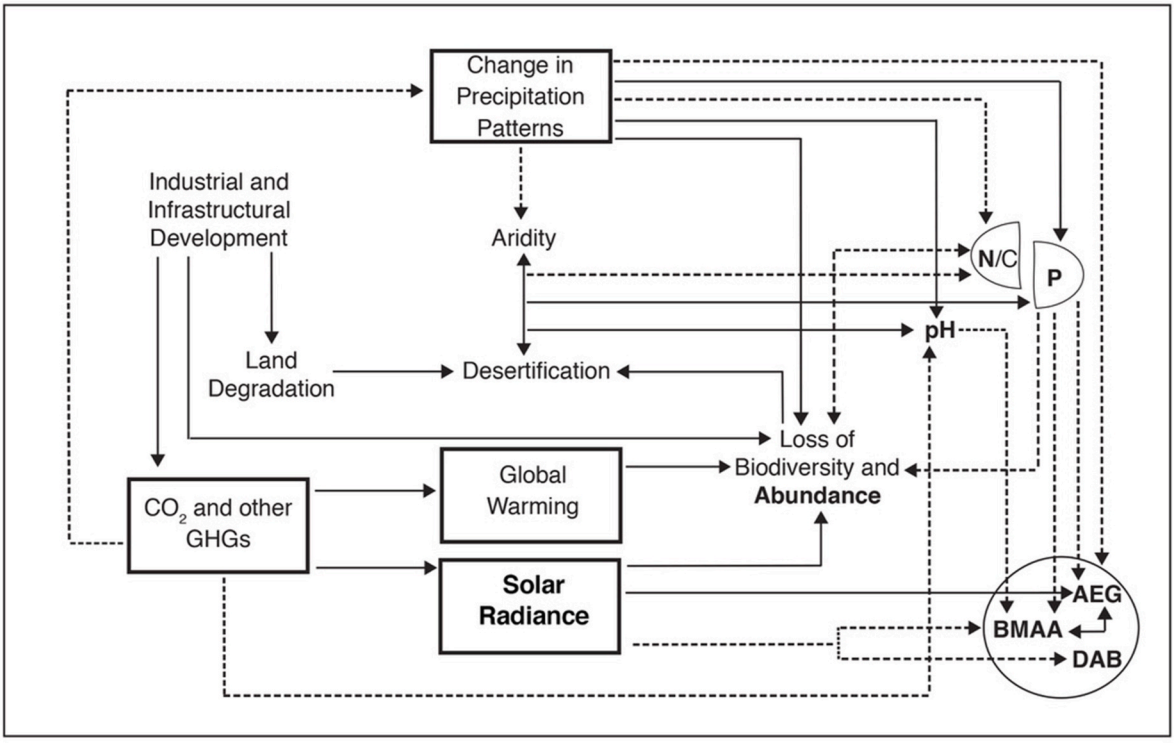

Fig. 4. Synthesis model of interacting forces that influence organismal abundance and toxin accumulation studied here (bold letters; Statistical Model 2). Positive interactions (solid lines) and negative interactions (dotted lines) are depicted between factors examined in this study (bold letters), and climate change-induced phenomena (thick boxes), nutrient cycling (half circles) and desertification. The toxins AEG, BMAA and DAB are enclosed in a circle to show that they exist in a common pool. Nitrogen to Carbon ratio (N/C) and Phosphorus (P) are depicted in half circles to denote that aridity decouples an otherwise coupled regulation of all three biogeochemical cycles. Solar forcing is used interchangeably with illumination. GHC: Greenhouse Gases.

photosynthesis, and carbon fixation which could further complicate these scenarios (Koksharova et al., 2020a, 2020b).

Global warming, already underway in Qatar where temperatures have risen by 1.6 °C since the 1950s (Berkley Earth, 2020) due to urbanization and fossil-fuel extraction, along with changes in precipitation patterns, can result in the loss of biodiversity and abundance and feed-forward to additional desertification (Fig. 4; Hori et al., 2011; Collins and Knutti, 2013; IPCC, 2019). In biocrusts, these phenomena cause the loss of late-successional dark-colored cyanobacteria, lichens and mosses returning to dominance the early successional light-colored cyanobacteria (Hori et al., 2011; MEA, 2005; Fernandes et al., 2018). The shift leads to an increase of albedo and a decrease in the absorption of solar radiance, otherwise absorbed by the dark-surfaced biocrusts, and warming of atmospheric temperatures ensues (Bell et al., 2005). In the scenario of increased solar radiance or illumination, cyanobacteria will respond to the stress by boosting the accumulation of AEG (Figs. 2 and 3). BMAA concentration may receive a boost by association, and DAB is predicted to decline (Figs. 2 and 3). Finally, if cloud covered days increase, based on our low illumination regime simulating such days, DAB and BMAA accumulation will peak, and by association AEG's (Table 1; Figs. 2 and 3).

5. Conclusion

Future studies are needed to decipher the function of these toxins in biocrust communities and to determine whether their production is influenced by the ecological interactions between cyanobacteria and their sympatric bacterial populations, and whether they bioaccumulate in the terrestrial food-chain in drylands. A more in-depth profiling of the microbial communities in biocrusts using a metagenomics approach, may further clarify species of dominance and toxin producers in biocrusts, and how this community's structure and composition change across environmental variable gradients and through time.

The wide variability in observations made across climates, ecosystems, and seasons, taken together with the differences between ecological hierarchies, suggests that toxin accumulation patterns do not conform to a simple set of predictors. Since the results so far appear to be regionally dependent and alterations to drylands affect one third of the world's population, it stands to reason that the scientific queries used to inform policy and regulations for human exposure protection and environmental protection should be regionally based as well. Finally, considering that desertification is a global-scale threat, drylands can serve as forecasters of near-future scenarios in temperate climate. This information can then be used to improve policies for nature conservation and regenerative development to protect against desertification.

Ethical statement

The authors wish to ensure that no part of this research work involved the use of human and non-human animal subjects. The research work was conducted ethically, transparently, and credit was assigned where it was owed.

CRediT authorship contribution statement

Aspassia D. Chatziefthimiou: Writing – review & editing, Writing – original draft, Visualization, Validation, Resources, Project administration, Methodology, Investigation, Formal analysis, Data curation, Conceptualization. **James S. Metcalf:** Writing – review & editing, Methodology, Formal analysis, Conceptualization, Visualization. **William B. Glover:** Writing – review & editing, Investigation. **James T. Powell:** Investigation. **Sandra A. Banack:** Writing – review & editing, Validation, Methodology, Investigation, Formal analysis. **Paul A. Cox:** Writing – review & editing, Resources, Methodology, Investigation, Funding acquisition, Conceptualization. **Moncef Ladjimi:** Writing – review & editing. **Ali A. Sultan:** Writing – review & editing. **Hiam Chemaitelly:** Writing – review & editing, Formal analysis. **Renee A. Richer:** Writing – review & editing, Resources, Investigation, Funding acquisition, Conceptualization.

Declaration of competing interest

The authors declare that they have no known competing financial interests or personal relationships that could have appeared to influence the work reported in this paper.

Data availability

Data shared

Acknowledgements

This publication was made possible by NPRP grant 4-775-1-116 from the Qatar National Research Fund (a member of Qatar Foundation), and a research scholarship to A.D.C. from the Qatar Natural History Group. The statements made herein are solely the responsibility of the authors. We thank the Deerbrook Charitable Foundation, the William Farrish Stamps Foundation, and Klara Farkas for funding support. We wish to thank Drs. Michel Louge and Anthony Hay for providing funding and support to A.D.C. We wish to acknowledge that Figs. 1 and 2 of this manuscript were created by Ms. Jenine Davidson. The authors would like to thank Chris Pieser for providing us the Chameleon Plasma Grow Light. We wish to acknowledge Dr. Laith Abu Raddad for his guidance in the statistical analysis and the services provided by the Biostatistics, Epidemiology, and Biomathematics Research Core at Weill Cornell Medicine-Qatar.

Appendix A. Supplementary data

Supplementary data to this article can be found online at https://doi.org/10.1016/j.toxcx.2024.100199.

References

Al-Sammak, M.A., Hoagland, K.D., Cassada, D., Snow, D.D., 2014. Co-occurrence of the cyanotoxins BMAA, DABA and Anatoxin-a in Nebraska Reservoirs, fish, and aquatic plants. Toxins 6, 488–508. https://doi.org/10.3390/toxins6020488.

Andersson, M.G.I., Berga, M., Lindström, E.S., Langenheder, S., 2014. The spatial structure of bacterial communities is influenced by historical environmental conditions. Ecology 95 (5), 1134–1140.

Banack, S.A., Downing, T.G., Spácil, Z., Purdie, E.L., Metcalf, J.S., Downing, S., Esterhuizen, M., Codd, G.A., Cox, P.A., 2010. Distinguishing the cyanobacterial neurotoxin β-N-methylamino-L-alanine (BMAA) from its structural isomer 2, 4-diaminobutyric acid (2, 4-DAB). Toxicon 56 (6), 868–879.

Banack, S.A., Metcalf, J.S., Jiang, L., Craighead, D., Ilag, L.L., Cox, P.A., 2012. Cyanobacteria produce N-(2-aminoethyl) glycine, a backbone for peptide nucleic acids which may have been the first genetic molecules for life on earth. PLoS One 7 (11), e49043.

Banack, S.A., 2021. Second laboratory validation of β-N-methylamino-L-alanine, N-(2aminoethyl) glycine, and 2, 4-diaminobuytric acid by ultra-performance liquid chromatography and tandem mass spectrometry. Neurotox. Res. 39 (1), 107–116.

Bell, T., Newman, J.A., Silverman, B.W., Turner, S.L., Lilley, A.K., 2005. The contribution of species richness and composition to bacterial services. Nature 436, 1157–1160. https://doi.org/10.1038/nature03891.

Belnap, J., 2003. The world at your feet: desert biological soil crusts. Front. Ecol. Environ. 1 (5), 181–189.

Belnap, J., Welter, J.R., Grimm, N.B., Barger, N., Ludwig, J.A., 2005. Linkages between microbial and hydrological processes in arid and semiarid watersheds. Ecology 86, 298e307.

Belnap, J., 2011. Biological phosphorus cycling in dryland regions. In: Bunemann, E.K., Oberson, A., Frossard, E. (Eds.), Phosphorus in Action, Soil Biology 26. Springer-Verlag, Berlin/Heidelberg, Germany, pp. 371–406. https://doi.org/10.1007/978-3-642-15271-9_15.

Berkley Earth, 2020. Global Temperature Report 2020.

Berntzon, L., Erasmie, S., Celepli, N., Eriksson, J., Rasmussen, U., Bergman, B., 2013. BMAA inhibits nitrogen fixation in the cyano-bacterium Nostoc sp. PCC 7120. Mar. Drugs 11, 3091–3108. https://doi.org/10.3390/md11083091.

Billi, D., Potts, M., 2002. Life and death of dried prokaryotes. Res. Microbiol. 153, 7–12.

Brand, L.E., Pablo, J., Compton, A., Hammerschlag, N., Mash, D.C., 2010. Cyanobacterial blooms and the occurrence of the neurotoxin beta-N-methylamino-L-alanine in South Florida aquatic food webs. Harmful Algae 9, 620–635.
Büdel, B., Colesie, C., Green, T.G.A., Grube, M., Suau, R.L., Loewen-Schneider, K., et al., 2014. Improved appreciation of the functioning and importance of biological soil crusts in Europe: the Soil Crust International Project (SCIN). Biodivers. Conserv. 23, 1639–1658. https://doi.org/10.1007/s10531-014-0645-2.
Carmichael, W.W., Gorham, P.R., 1978. Anatoxins from clones of Anabaena flos-aquae isolated from lakes of western Canada. Mitt. Int. Ver. Theor. Angew. Limnol. 21, 285–295.
Castenholz, R.W., Garcia-Pichel, F., 2000. Cyanobacterial responses to UV-radiation. In: Whitton, B.A., Potts, M. (Eds.), Ecology of Cyanobacteria: Their Diversity in Time and Space. Kluwer Academic Publishers, pp. 591–611.
Chatziefthimiou, A.D., Richer, R., Rowles, H., Powell, J.T., Metcalf, J.S., 2014. Cyanotoxins as a potential cause of dog poisonings in desert environments. Vet. 174, 484–485.
Chatziefthimiou, A.D., Metcalf, J.S., Glover, W.B., Banack, S.A., Dargham, S.R., Richer, R.A., 2016. Cyanobacteria and cyanotoxins are present in drinking water impoundments and groundwater wells in desert environments. Toxicon 114, 75–84. https://doi.org/10.1016/j.toxicon.2016.02.016.
Chatziefthimiou, A.D., Deitch, D.J., Glover, W.B., Powell, J.T., Banack, S.A., Richer, R.A., et al., 2018. Analysis of neurotoxic amino acids from marine waters, microbial mats and seafood destined for human consumption in the Arabian Gulf. Neurotox. Res. 33 (1), 143–152. https://doi.org/10.1007/s12640-017-9772-3.
Chatziefthimiou, A.D., Banack, S.A., Cox, P.A., 2020. Biocrust-produced cyanotoxins are found vertically in the desert soil profile. Neurotox. Res. 39, 42–48. https://doi.org/10.1007/s12640-020-00224-x.
Cirés, S., Casero, M.C., Quesada, A., 2017. Toxicity at the edge of life: a review on cyanobacterial toxins from extreme environments. Mar. Drugs 15, 233. https://doi.org/10.3390/md15070233.
Collins, M., Knutti, R., 2013. Long-term climate change: projections, commitments and irreversibility. In: Stocker, T.F., Qin, D., Plattner, G.-K., Tignor, M., Allen, S.K., Boschung, A., et al. (Eds.), Climate Change 2013 Physical Science Basis Contribution to the Working Group I to Fifth Assessment Report of the Intergovernmental Panel on Climate Change. Cambridge University Press, Cambridge, UK, pp. 1029–1136. https://doi.org/10.1017/CBO9781107415324.0241007/s12640-017-9772-3.
Conell, J.H., 1978. Diversity in tropical rain forests and coral reefs. Science 199 (4335), 1302–1310.
Cox, P.A., Banack, S.A., Murch, S.J., 2003. Biomagnification of cyanobacterial neurotoxins and neurodegenerative disease among the Chamorro people of Guam. Proc. Natl. Acad. Sci. USA 100, 13380–13383.
Cox, P.A., Banack, S.A., Murch, S.J., Rasmussen, U., Tien, G., Bidigare, R.R., Metcalf, J.S., Morrison, L.F., Codd, G.A., Bergman, B., 2005. Diverse taxa of cyanobacteria produce β-N-methylamino-L-alanine, a neurotoxic amino acid. Proc. Natl. Acad. Sci. USA 102 (14), 5074–5078.
Cox, P.A., Richer, R., Metcalf, J.S., Banack, S.A., Codd, G.A., Bradley, W.G., 2009. Cyanobacteria and BMAA exposure from desert dust—a possible link to sporadic ALS among Gulf War Veterans. Amyotroph Lateral Scler. 10 (S2), 109–117.
Cox, P.A., Davis, D.A., Mash, D.C., Metcalf, J.S., Banack, S.A., 2016. Dietary exposure to an environmental toxin triggers neurofibrillary tangles and amyloid deposits in the brain. Proc Royal Soc B 283, 2397. https://doi.org/10.1098/rspb.2015.2397.
Davis, D.A., Cox, P.A., Banack, S.A., Lecusay, P.D., Garamszegi, S.P., Hagan, M.J., et al., 2020. L-serine reduces spinal cord pathology in a vervet model of preclinical ALS/MND. JNEN (J. Neuropathol. Exp. Neurol.) 79 (4), 393–406.
Delgado-Baquerizo, M., Maestre, F.T., Gallardo, A., Bowker, M.A., Wallenstein, M.D., Quero, J.L., et al., 2013. Decoupling of soil nutrient cycles as a function of aridity in global drylands. Nature 502, 672–676. https://doi.org/10.1038/nature12670.
Dörr, F.A., Rodríguez, V., Molica, R., Henriksen, P., Krock, B., Pinto, E., 2010. Methods for detection of anatoxin-a(*S*) by liquid chromatography coupled to electrospray ionization-tandem mass spectrometry. Toxicon 55 (1), 92–99.
Downing, S., Banack, S.A., Metcalf, J.S., Cox, P.A., Downing, T.G., 2011. Nitrogen starvation of cyanobacteria results in the production of b-Nmethyloamino-Lalanine. Toxicon 58, 187e194.
Downing, S., van de Venter, M., Downing, T.G., 2012. The Effect of exogenous β-N-Methylamino-L-alanine on the growth of Synechocystis PCC6803. Microb. Ecol. 63, 149–156.
Downing, T.G., Phelan, R.R., Downing, S., 2015. A potential physiological role for cyanotoxins in cyanobacteria of arid environments. J. Arid Environ. 112 (Part B), 147–151.
Dulić, T., Meriluoto, J., Palanački Malešević, T., Gajić, V., Važić, T., Tokodi, N., Obreht, I., Kostić, B., Kosijer, P., Khormali, F., Svirčev, Z., 2017. Cyanobacterial diversity and toxicity of biocrusts from the Caspian Lowland loess deposits, North Iran. Quat. Int. 429 (Part B), 74–85. https://doi.org/10.1016/j.quaint.2016.02.046.
Dulić, T., Svirčev, Z., Palanački Malešević, T., Faassen, E.J., Savela, H., Hao, Q., Meriluoto, J., 2022. Assessment of common cyanotoxins in cyanobacteria of biological loess crusts. Toxins 14, 215. https://doi.org/10.3390/toxins14030215.
Evans, R.D., Belnap, J., Garcia-Pichel, F., Phillips, S.L., 2001. Global change and the future of biological soil crusts. In: Belnap, J., Lange, O.L. (Eds.), Biological Soil Crusts: Structure, Function, and Management. Springer-Verlag Berlin, Berlin/Heidelberg, Germany, pp. 417–429.
Faist, A.M., Herrick, J.E., Belnap, J., Van Zee, J.W., Barger, N.N., 2017. Biological soil crust and disturbance controls on surface hydrology in a semi-arid ecosystem. Ecosphere 8 (3), e01691.
Fan, H., Qiu, J., Fan, L., Li, A., 2015. Effects of growth conditions on the production of neurotoxin 2,4-diaminobutyric acid (DAB) in Microcystis aeruginosa and its universal presence in diverse cyanobacteria isolated from freshwater in China. Environ. Sci. Pollut. Res. Int. 22 (8), 5943–5951. https://doi.org/10.1007/s11356-014-3766-y.
Fastner, J., Flieger, I., Neumann, U., 1998. Optimised extraction of microcystins from field samples: a comparison of different solvents and procedures. Water Res. 32, 3177–3181.
Fernandes, V.M.C., Machado de Lima, N.M., Roush, D., Rudgers, J., Collins, S.L., Garcia-Pichel, F., 2018. Exposure to predicted precipitation patterns decreases population size and alters community structure of cyanobacteria in biological soil crusts from the Chihuahuan Desert. Environ. Microbiol. 20 (1), 259–269. https://doi.org/10.1111/1462-2920.13983.
Ferrenberg, S., Reed, S.C., Belnap, J., 2015. Climate change and physical disturbance cause similar community shifts in biological soil crusts. Proc. Natl. Acad. Sci. USA 112 (39), 12116–12121. https://doi.org/10.1073/pnas.1509150112.
Fierer, N., Jackson, R.B., 2006. The diversity and biogeography of soil bacterial communities. Proc. Natl. Acad. Sci. USA 103 (3), 626–631.
Fiore, M.F., de Lima, S.T., Carmichael, W.W., McKinnie, S.M.K., Chekan, J.R., Moore, B. S., 2020. Guanitoxin, re-naming a cyanobacterial organophosphate toxin. Harmful Algae 92, 101737. https://doi.org/10.1016/j.hal.2019.101737.
Garcia-Pichel, F., Johnson, S.L., Youngkin, D., Belnap, J., 2003. Small-scale vertical distribution of bacterial biomass and diversity in Biological Soil Crusts from arid lands in the Colorado Plateau. Microb. Ecol. 46, 312–321. https://doi.org/10.1007/s00248-003-1004-0.
Hori, Y., Stuhlberger, C., Simonett, O., 2011. Desertification: a Visual Synthesis. United Nations Convention to Combat Desertification (UNCCD).
Horner, R.D., Kamins, K.G., Feussner, J.R., Grambow, S.C., Hoff-Lindquist, J., Harati, Y., et al., 2003. Occurrence of amyotrophic lateral sclerosis among Gulf War veterans. Neurology 61, 742–749.
IPCC, 2019. Climate Change and Land. In: on climate change, desertification, land degradation, sustainable land management, food security, and greenhouse gas fluxes in terrestrial ecosystems. an IPCC special, Cambridge, UK and New York, NY, USA, p. 896 https://doi.org/10.101/9781009157988.
Jiao, Y., Chen, Q., Chen, X., Wang, X., Liao, X., Jiang, L., et al., 2014. Occurrence and transfer of a cyanobacterial neurotoxin β-methylamino-l-alanine within the aquatic food webs of Gonghu Bay (Lake Taihu, China) to evaluate the potential human health risk. Sci. Total Environ. 468–469, 457–463.
Jonasson, S., Eriksson, J., Berntzon, L., Spáčil, Z., Ilag, L.L., Ronnevi, L.-O., et al., 2010. Transfer of a cyanobacterial neurotoxin within a temperate aquatic ecosystem suggested pathways for human exposure. Proc. Natl. Acad. Sci. USA 107, 9252–9257.
Koksharova, O.A., Butenko, I.O., Pobeguts, O.V., Safronova, N.A., Govorun, V.M., 2020a. The first proteomic study of Nostoc sp. PCC 7120 exposed to cyanotoxin BMAA under nitrogen starvation. Toxins 12, 310. https://doi.org/10.3390/toxins12050310.
Koksharova, O.A., Butenko, I.O., Pobeguts, O.V., Safronova, N.A., Govorun, V.M., 2020b. Proteomic insights into starvation of nitrogen-replete cells of Nostoc sp. PCC7120 under BMAA treatment. Toxins 12, 372. https://doi.org/10.3390/toxins12060372.
Kormas, K.A., Lymperopoulou, D.A., 2013. Cyanobacterial toxin degrading bacteria: who are they? BioMed Res. Int. 2013, 463894 https://doi.org/10.1155/2013/463894.
Lage, S., Annadotter, H., Rasmussen, U., Rydberg, S., 2015. Biotransfer of β-N Methylamino-L-alanine (BMAA) in a eutrophicated freshwater lake. Mar. Drugs 13, 1185–1201. https://doi.org/10.3390/md13031185.
Lal, R., 2011. Soil health and climate change: an overview. In: Singh, B.P., Cowie, A.L., Chan, K.Y. (Eds.), Soil Health and Climate Change, Soil Biology, vol. 29. Springer-Verlag, Berlin, Germany, pp. 3–24. https://doi.org/10.1007/978-3-642-20256-8_1.
Lindström, E.S., Langenheder, S., 2012. Minireview: local and regional factors influencing bacterial community assembly. Environmental Microbiology Reports 4, 1–9.
Liu, L., Xing, Z., Yang, H., 2017. Effect of biological soil crusts on microbial activity in soils of the Tengger Desert (China). J. Arid Environ. 144, 201–211.
Loreau, M., Naeem, S., Inchausti, P., Bengtsson, J., Grime, J.P., Hector, A., et al., 2001. Biodiversity and ecosystem functioning: current knowledge and future challenges. Science 294, 804–808. https://doi.org/10.1126/science.1064088.
Luomi, M., 2016. The Gulf Monarchies and Climate Change: Abu Dhabi and Qatar in an Era of Natural Unsustainability. C Hurst and Co Publishers Ltd., London, UK.
Maestre, F.T., Salguero-Gómez, R., Quero, J.L., 2012. It is getting hotter in here: determining and projecting the impacts of global environmental change on drylands. Phil Trans R Soc B 367, 3062–3075. https://doi.org/10.1098/rstb.2011.0323.
McDonald, J.F., Moffit, R.A., 1980. The uses of tobit analysis. Rev. Econ. Stat. 62 (2), 318–321.
Mahmood, N.A., Carmichael, W.W., 1987. Anatoxin-a(*S*), an anticholinesterase from the cyanobacterium *Anabaena flos-aquae* NRC-525-17. Toxicon 25, 1221–1227.
Martin, R.M., Stallrich, J., Bereman, M.S., 2019. Mixture designs to investigate adverse effects upon co-exposure to environmental cyanotoxins. Toxicology 421, 74–83.
MDPS (Ministry of Development Planning and Statistics), 2017. Environment Statistics Report 2017.
MEA, 2005. Ecosystems and Human Well-Being: Desertification Synthesis. World Resources Institute, Washington, DC, USA.
Mergeay, J., De Meester, L., Eggermont, H., Verschuren, D., 2011. Priority effects and species sorting in along paleoecological record of repeated community assembly through time. Ecology 92, 2267–2275.
Metcalf, J.S., Morrison, L.F., Krienitz, L., Ballot, A., Krause, E., Kotut, K., et al., 2006. Analysis of the cyanotoxins anatoxin-a and microcystins in Lesser Flamingo feathers. Toxicol. Environ. Chem. 88, 159–167.
Metcalf, J.S., Codd, G.A., 2012. Cyanotoxins. In: Whitton, B.A. (Ed.), In Ecology of Cyanobacteria II: Their Diversity in Time and Space. Springer, New York, NY, pp. 651–675.

Metcalf, J.S., Richer, R., Cox, P.A., Codd, G.A., 2012. Cyanotoxins in desert environments may present a risk to human health. Sci. Total Environ. 421–422, 118–123.
Metcalf, J.S., Banack, S.A., Richer, R., Cox, P.A., 2015. Neurotoxic amino acids and their isomers in desert environments. J. Arid Environ. 112, 140–144. https://doi.org/10.1016/j.jaridenv.2014.08.002.
MMAA (Ministry of Municipal Affairs and Agriculture), 2005. The Atlas of Soils for the State of Qatar - Soil Classification and Land Use Specification Project for the State of Qatar. Doha.
MOE (Ministry of Environment), 2014. Hydro-Meteorological Yearbook 2013-2014.
Molica, R.J.R., Oliveira, E.J.A., Carvalho, P.V.V.C., Costa, A.N.S.F., Cunha, M.C.C., Melo, G.L., Azevedo, S.M.F.O., 2005. Occurrence of saxitoxins and an anatoxin-a(S)-like anticholinesterase in a Brazilian drinking water supply. Harmful Algae 4, 743–753.
Paerl, H.W., Huisman, J., 2009. Climate change: a catalyst for global expansion of harmful cyanobacterial blooms. Environmental Microbiology Reports 1 (1), 27–37.
Pepe-Ranney, C., Koechli, C., Potrafka, R., Andam, C., Eggleston, E., Garcia-Pichel, F., et al., 2015. Non-cyanobacterial diazotrophs mediate dinitrogen fixation in biological soil crusts during early crust formation. ISME J. 10 (2), 1–12.
Perez-Astudilloa, D., Bachour, D., 2014. DNI, GHI and DHI ground measurements in Doha, Qatar. Energy Proc. 49, 2398–2404.
Popova, A., Rasmussen, U., Semashko, T., Govorun, V., Koksharova, O., 2018a. Stress effects of cyanotoxin β-methylamino-L-alanine (BMAA) on cyanobacterial heterocyst formation and functionality. Environmental Microbiology Reports 10, 369–377. https://doi.org/10.1111/1758-2229.12647.
Popova, A., Semashko, T., Kostina, N., Rasmussen, U., Govorun, V., Koksharova, O., 2018b. The cyanotoxin BMAA induces heterocyst specific gene expression in Anabaena sp. PCC 7120 under repressive conditions Toxins 10, E478. https://doi.org/10.3390/toxins10110478.
Powell, J.T., Chatziefthimiou, A.D., Banack, S.A., Cox, P.A., Metcalf, J.S., 2015. Desert crust microorganisms, their environment, and human health. J. Arid Environ. 112 (Part B), 127–133.
Prăvălie, R., 2016. Drylands extent and environmental issues. A global approach. Earth Sci. Rev. 161, 259–278. https://doi.org/10.1016/j.earscirev.2016.08.003.
QMD (Qatar Meteorology Department), 2021. Climate data. https://www.caa.gov.qa/en-us/Pages/Metrogical.aspx#. (Accessed 13 October 2021).
Raggio, J., Green, T.G.A., Sancho, L.G., Pintado, A., Colesie, C., Weber, B., et al., 2017. Metabolic activity duration can be effectively predicted from macroclimatic data for biological soil crust habitats across Europe. Geoderma 306, 10–17.
Richer, R., Anchassi, D., El-Assaad, I., El-Matbouly, M., Ali, F., Makki, I., et al., 2012. Variation in the coverage of biological soil crusts in the State of Qatar. J. Arid Environ. 78, 187–190.
Richer, R., Banack, S.A., Metcalf, J.S., Cox, P.A., 2015. The persistence of cyanobacterial toxins in desert soils. J. Arid Environ. 112, 134–139.
Rippka, R., 1988. Isolation and purification of cyanobacteria. Methods Enzymol. 167, 3–27.
Rockström, J., Steffen, W., Noone, K., Persson, Å., Chapin, F.S., Lambin, E.F., et al., 2009. A safe operating space for humanity. Nature 461 (7263), 472–475.
Rutherford, W.A., Painter, T.H., Ferrenberg, S., Belnap, J., Okin, G.S., Flagg, C., et al., 2017. Albedo feedbacks to future climate via climate change impacts on dryland biocrusts. Sci. Rep. 7, 44188 https://doi.org/10.1038/srep44188.
Schmidt, S.K., Nemergut, D.R., Darcy, J.L., Lynch, R., 2014. Do bacterial and fungal communities assemble differently during primary succession? Mol. Ecol. 23, 254–258.
Schneider, T., Simpson, C., Desai, P., Tucker, M., Lobner, D., 2020. Neurotoxicity of isomers of the environmental toxin L-BMAA. Toxicon 1 (184), 175–179.
SCOR, 1966. Determination of photosynthetic pigments in seawater. UNESCO Monographs on Oceanographic Methodology 1, 11–18. UNESCO.
SSE (Surface meteorology and Solar Energy – NASA), 2017. Atmospheric Science Data Center. https://eosweb.larc.nasa.gov/sse/.
StataCorp, 2013. Stata Statistical Software/SE: Release 13. StataCorp LP: College Station, TX, USA.
Stommel, E.W., Field, N.C., Caller, T.A., 2013. Aerosolization of cyanobacteria as a risk factor for amyotrophic lateral sclerosis. Med. Hypotheses 80 (2), 142–145.
Urban, M.C., De Meester, L., 2009. Community monopolization: local adaptation enhances priority effects in an evolving metacommunity. Proc. R. Soc. A B 276, 4129–4138. https://doi.org/10.1098/rspb.2009.1382.
Ward, C.J., Beattie, K.A., Lee, E.Y.C., Codd, G.A., 1997. Colorimetric protein phosphatase inhibition assay of laboratory strains and natural blooms of cynobacteria: comparisons with high performance liquid chromatographic analysis for microcystins. FEMS Microbiol. Letters 153, 465–473.
Whitton, B.A., 2002. Phylum cyanophyta (cyanobacteria). In: John, D.M., Whitton, B.A., Brook, A.J. (Eds.), The Freshwater Algal Flora of the British Isles. Cambridge University Press, Cambridge, UK, pp. 25–122.
WMO (World Meteorological Organization), 2018. WMO Statement on the State of the Global Climate in 2018. WMO-No.1233.